Airborne Algal Growth on the Roofs of Membrane-Structured Residences in Cold Areas of Japan

Makiko Nakajima[1], Daisuke Masueda[1], Shuichi Hokoi[2] and Takayuki Matsushita[1]

[1] Department of Architecture, Graduate School of Engineering, Kobe University, 1-1 Nada-ku, Kobe, 657-8501, Japan, nakajima@gold.kobe-u.ac.jp

[2] Southeast University, Sipailou 2#, Nanjing, 210096, P. R. China, hokoi@seu.edu.cn

Abstract. *Discoloration of building facades due to airborne algae is observed in our surroundings. The growth conditions of these algae are not fully clear yet, and efficient preventive measures have not yet been determined. This study was aimed at investigating the influence of ambient environment and building structure on algal growth. A residential building in the cold region of Japan was surveyed. The roof was a multilayered structure consisting of a semi-transparent film, an air layer, an outside insulation layer, and was supported by rafters. The soiled state was visually observed and recorded through pictures, and seemed to be particularly increased in autumn. Several black stripes appeared on the northeast (NE) roof four months after its cleaning. The soiling first appeared on the film backed by the rafter, and then extended to the film backed by the air layer. It rarely appeared on the southeast roof. The roof-surface temperature was measured and a stripe-shaped distribution was observed. The temperature of the film with rafter was higher and lesser than that of the film with the air layer during the night and in the early morning, respectively. Although condensation occurred nightly, its frequency showed no orientational difference. Algae can die when exposed to a temperature higher than 40 °C. The southwest roof had the longest period of a surface temperature over 40 °C, while the northwest (NW) roof had the shortest period of this surface temperature. These measurements corresponded well to the survey results according to which soiling mainly occurred on the NE and NW sides of roofs. The time for algal growth was estimated assuming that algae can grow at surface temperatures between 0 and 40 °C.*

Keywords: *Roof Soiling, Airborne Algae, Surface Temperature, Condensation, Membrane Structure.*

1 Introduction

An observation of the exterior walls of building walls shows many black or/and green soiling. Some studies showed that this is caused by the adhesion and growth of airborne algae. Currently, the main countermeasures against the algal soling are cleaning and repainting of such walls; however, efficient preventive measures have not been developed yet.

Sharma et al. showed that airborne algae reported to date are species of 103 classes of the three divisions. Tsujimoto et al. investigated the algal soiling in Japan and showed that algal soiling could occur in all Japanese climatic zones. Häubner et al. showed that *Stichococcus* sp. and *Chlorella luteoviridis* could grow at 1–35 °C, and their growth rate increases with increasing temperature and reaches the maximum at 10–25 °C and is nonexistent at 30–35 °C. Agrawal et al. showed that the survival rate of algae is greatly reduced when algae are exposed to high temperatures over 40 °C for several tens of minutes. Nakajima et al. surveyed the soiling conditions of a building with respect to the surrounding environment and showed that algae could grow even on walls rarely exposed to rainwater when the humidity is high and if

temperatures remained below 40 °C. They thus proposed a predictive model of the algal growth and death on exterior walls as a function of the solar radiation, temperature, and humidity.

Although several studies have shown the qualitative relationship between airborne algal growth and the environment, their quantitative relationship has not been fully evaluated yet. This study was aimed at determining this relationship by focusing on a residential building with membrane-structured roofs in a cold region of Japan.

## 2 Method of Survey and Measurements

2.1 Overview of Measured Building and Climatic Conditions

The one-story residential building that was considered for this study is located in Taiki town, Hokkaido, Japan, and is surrounded by open grassland. It has a hipped roof structure, with rafters arranged at intervals of 40 cm and insulations packed between them (Figures 1a and 1b). The part with a thermal insulation layer has a cross section with a six-layer structure comprising an exterior film, an outside air layer, the thermal insulation, a vapor-barrier, an inside air layer, and the glass cloth, from the outside (Figure 1c). All the materials are semi-transparent. The exterior film is made of a vinyl chloride film and a polyester base fabric and coated by fluororesin.

Taiki town is located close to the sea and has subarctic climate. Figure 2 provides a graphical representation of the outdoor temperature, relative humidity, and precipitation. The daily average temperature falls below freezing point in winter but rises to approximately 20 °C in summer. The relative humidity is over 80% in summer.
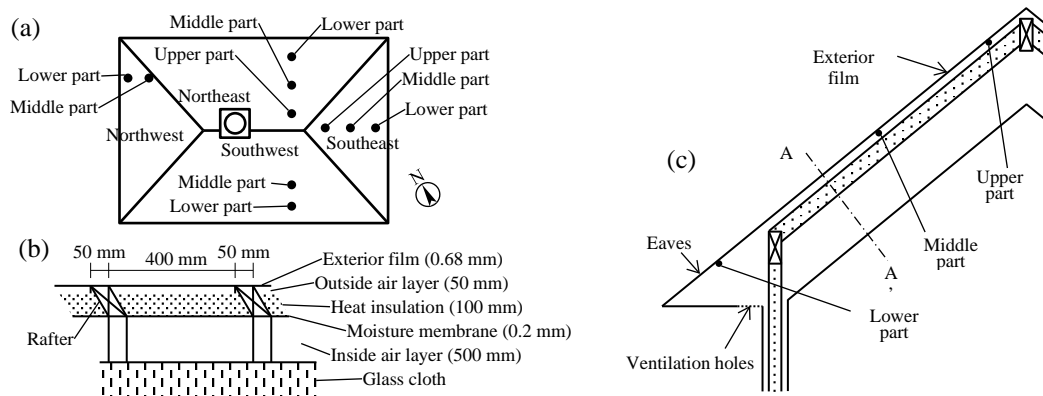
Figure 1. Overview of the measured house: (a) roof plan, (b) A–A' section of roof in (c), and (c) vertical section of the roof.
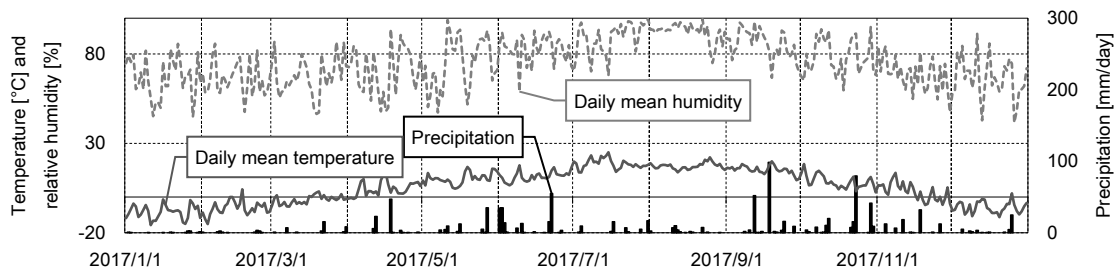
Figure 2. Outdoor temperature, relative humidity, and precipitation in Taiki Town, Hokkaido, Japan.

2.2 Measurement of Roof Surface Temperatures and Climatic Conditions

The surface temperatures of the roofs were measured through thermocouples and hygrothermal sensors. The thermocouples were fixed to the indoor side of the exterior film by tape, and the measured values were regarded as the surface temperatures because the film thickness was very thin at 0.68 mm. The surface temperature was measured at the upper, middle, and lower parts on the NE and southeast (SE) roofs, and at the middle and lower parts on the NW and southwest (SW) roofs, as shown in Figure 1a.

The outdoor temperature and humidity were measured by a thermometer and hygrometer (U23-002, Onset Computer Corporation), respectively, about 5-m NW to the building, where the vertical and horizontal global solar radiations were measured through pyrheliometers (ML-01, EKO Instruments).

2.3 Survey on Roof Soiling

The soiling of roofs was recorded through photographs captured by fixed-point cameras set around the building on September 2017; the NE, NW, and SE roofs were photographed every 4 h.

3 Surveyed and Measured Results

3.1 Soiling of Roof Surface

3.1.1 Soiling difference depending on roof orientation

The photos of each roof are shown in Figure 3. The stripe-shaped soiling extends vertically from the top to the bottom in the center of the NE roof. In the same manner, the stripe-shaped soiling is also generated in the center of the NW roof. The soiling cannot be seen on the SE and SW roofs.
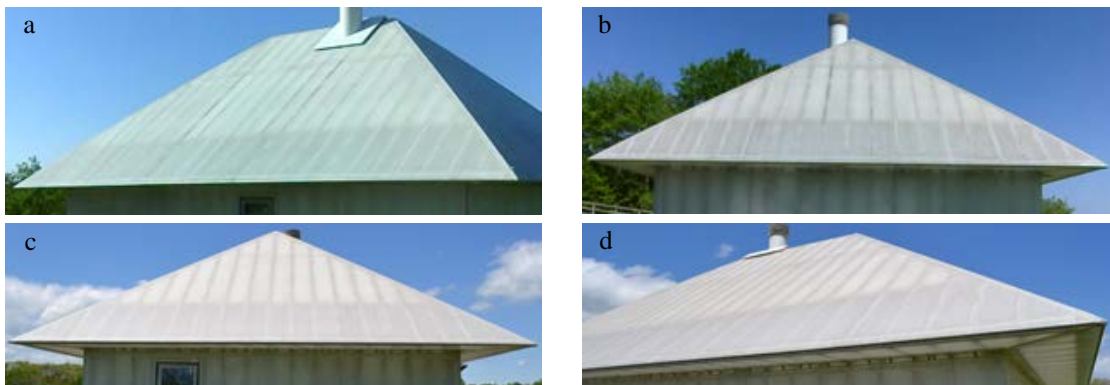
Figure 3. Photographs of (a) NE roof, (b) NW roof, (c) SE roof, and (d) SW roof on May 2018.

3.1.2 Time profiles of soiling on NE and NW roofs

The photos of the NE and NW roofs from September 19, 2017 to March 19, 2019 are shown in Figures 4 and 5, respectively. The roofs were cleaned by brushing and high-pressure washing

on April 4, 2017, after which soiling was not observed on July 5, 2017. The soiling occurred again at the mid-left part of the NE roof on September 19, 2017, and was observed on the roof part downward from the chimney on October 20, 2017. On November 18, 2017, the soiling darkened but did not show further change until December 15, 2017. The soiling on the eaves faded on May 27, 2018, then became darker between June 21 and July 26, 2018. On August 26, 2018, the soiled area increased, the color darkened more than that on July 26, and gradually darkened further from September 22 to October 15, 2018. The roofs were cleaned again on October 22, 2018, after which soiling occurred at the left part of the roof downward from the chimney on November 19, 2018; this remained unchanged from December 23, 2018 to January 23, 2019. The stripe-shaped soiling increased in the area downward from the chimney and darkened on March 19, 2019.

In summary, the soiling hardly increased in the summer (July and August) and winter (December, January, and February) but increased from March to June and from September to November. The NW and NE roofs showed the same soiling tendencies.

**Figure 4.** Photographs of NE roof from September 2017 to March 2019.

Figure 5. Photographs of NW roof from September 2017 to February 2019.

3.1 Surface Temperature of Roofs

### 3.2.1 *Difference in film temperature between parts backed by rafter and air layer*

The surface temperature of the NE roof in summer and winter is shown in Figure 6. In summer, the temperature of the film backed by the rafter (hereafter referred to as rafter part) was almost the same as that of the film backed by the air layer (air layer part) (Figure 6a). The temperature of the rafter part was approximately 1 °C higher than that of the air layer part during the daytime, and the temperatures of both were almost the same at night. In winter, the temperature of the air layer part was 3–5 °C higher than that of the rafter part in the daytime and 1–2 °C higher at night (Figure 7a).
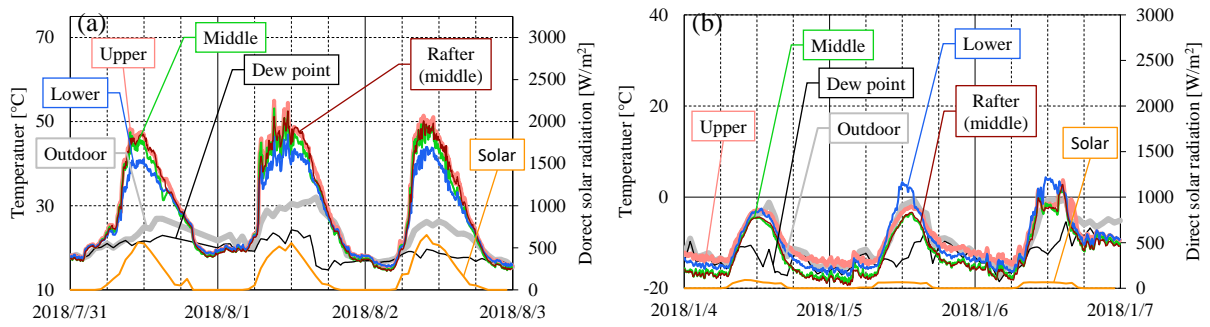
Figure 6. Direct solar radiation and surface temperatures of NE roof in (a) summer and (b) winter.

3.2.2 *Annual change in surface temperature on each roof*

The annual surface temperature on the NE and SW roofs is shown in Figure 7, where high temperatures of over 45 °C can be observed from June to August on the NE roof, and from February to December on the southwest roof. On the NE roof, where the incident direct solar radiation was the least, the frequency of temperature higher than 45 °C was least (Figure 7a). The daily fluctuation of the surface temperature was large on the SW roofs (Figure 7b).
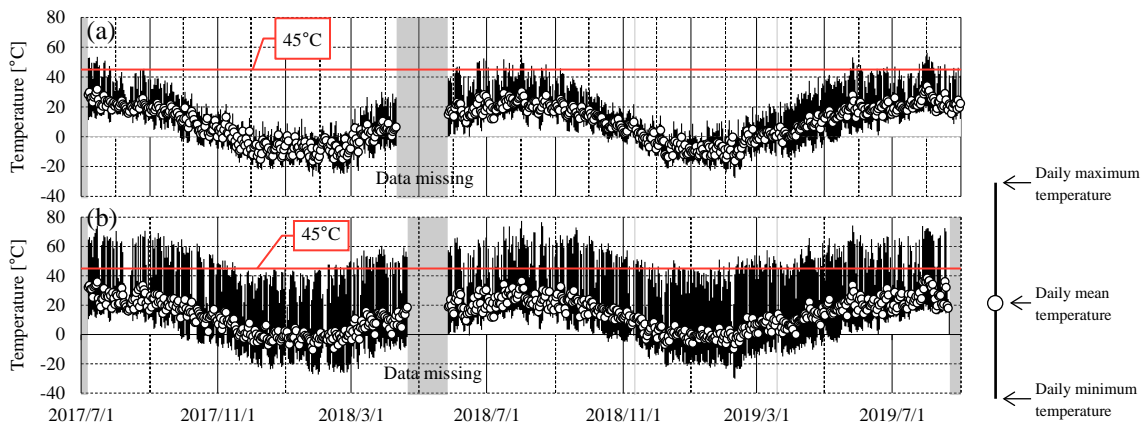
Figure 7. Annual surface-temperature change on (a) the NE and (b) SW roofs. The bar length and circles represent the daily-temperature difference and daily mean temperature, respectively.

3 Discussion

3.1 Relationship between Roof Surface Temperature and Roof Structure

In general, the roof surface temperature is higher at the upper part than at the lower parts (Figures 6). This is probably because the outside air layer was warmed by solar radiation, leading to thermal stratification. This stratification is likely to be accelerated by the nonuniform structure of the roof. The upper and middle parts comprise the air layer of 50-mm thickness and a 100-mm-thick insulating material, while the lower part does not have thermal insulation. Therefore, the air volume at the upper and middle parts was smaller than that at the lower part and their heat capacities were smaller.

5

4.2 Surface Condensation on Roof

Figure 8 shows the time when the surface temperature was below the dew-point temperature of the outdoor air. Frost was assumed to occur when the surface temperature was below 0 °C. As shown in Figures 6, the surface temperatures on all roofs decreased below the dew-point temperature of the outdoor air because of the nocturnal radiation, and they dropped below 0 °C at night from November to April. Condensation occurred from May to October, and condensation per day was long especially from September to October. This period of condensation differs depending on the roof orientation; however, the frequency of occurrence shows only a very small dependence on the orientation.
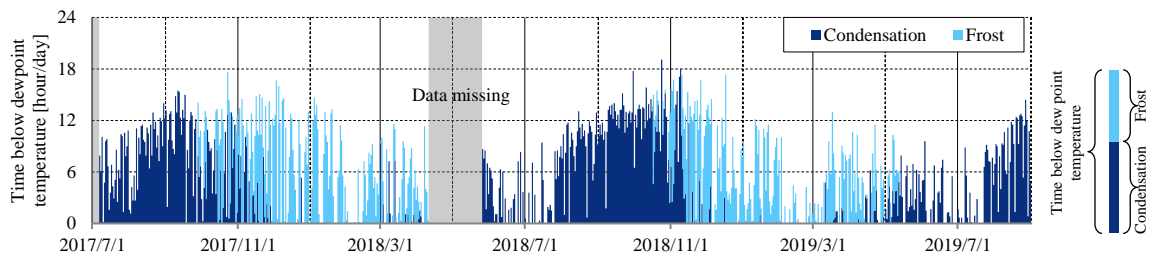
Figure 8. Time per day that the surface temperature was below the dew-point temperature of the outdoor air. Air-layer part at middle part of NE roof.

4.3 Dependence of Soiling on Roof Orientation

The soiling situation at the surveyed building was evaluated by focusing on the surface temperature and available water (condensation). Algae can grow in the temperature range of 1–30 °C, and they die when exposed to the high temperatures. Thus, we focused on the occurrence frequency of high temperatures of over 45°C.

On all the roofs, the surface condensation occurred (the source of water supply to the algae) at night from May to November. Therefore, the algae can grow from May to November.

The measured roof temperatures showed that the SW, SE, NW, and NE roofs, in this order, show high temperature frequency of over 45 °C. From May to November, the surface condensation on the SE and SW roofs occurred during the night but was over 45 °C almost every day. Therefore, the algae are considered to die because of high temperatures during daytime, and soiling did not occur despite sufficient water supply. Compared to all roofs, the frequency of the high temperature of over 45 °C was least on the NE roof when surface condensation occurred, and thus the algae grew most actively on this roof. These results correspond well to the surveyed results where soiling was observed to occur on the NE and NW roofs but not on the SE and SW roofs (Figure 3).

4.4 Difference between Soiling on Rafter and Air-Layer Parts

For the rafter and air-layer parts of the NE roof, the frequency of high temperatures of over 45 °C was almost same. However, the surface condensation on the rafter part occurred more frequently than on the air-layer part, and the condensation period per day was longer on the rafter part from March to November. Therefore, the algae are considered to grow more likely at the rafter part than at the air part (Figure 3).

6

4.5 Occurrence of Soiling Based on Time of Year

Considering the water supply and temperature suitable for algal growth, the estimated time of the year when the algae can survive is shown in Figure 9. For example, on the NE roof, the surface temperatures were from 0 to 45 °C and condensation occurred from August to September 2017, the middle of July 2018, and from September to October 2018. Thus, the algae are predicted to grow during these periods. This prediction corresponds well to the result that the soiling was observed from July to November 2017 and from June to November 2018, as shown in Figure 4.

On the SW roof, the high temperatures of over 45 °C occurred all year round. Therefore, it is predicted that the algae could grow only in a limited time in February 2017, from the end of November to the beginning of December 2017, and a part of January 2018. These predictions well correspond to the observed result that soiling did not occur on the SW roofs.
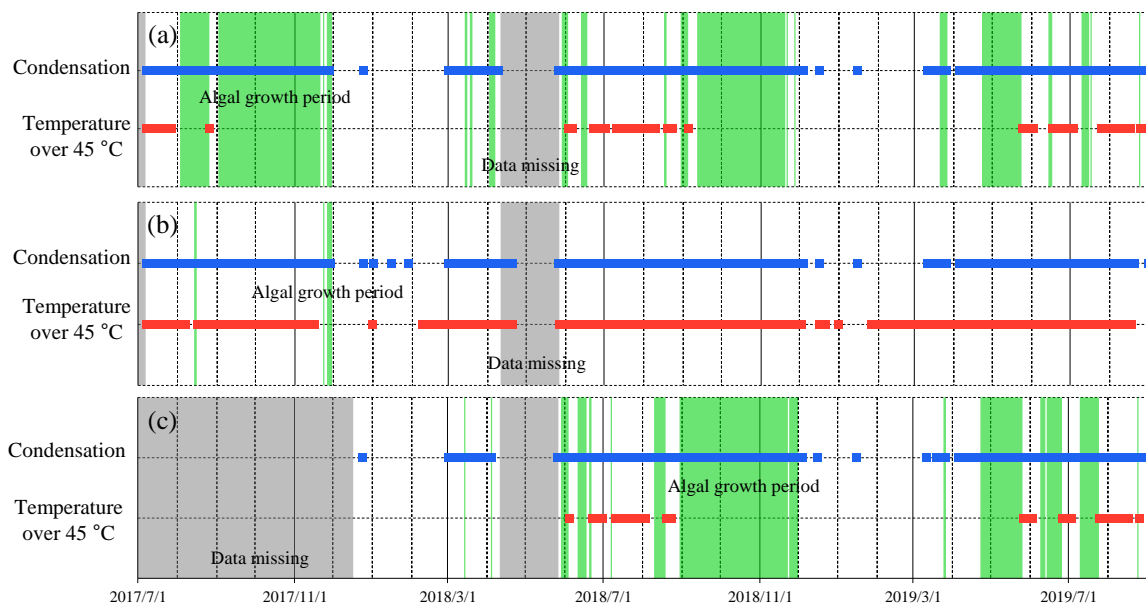
Figure 91. Estimated period for algal growth because of the occurrence of the condensation and high temperature. Air-layer part of middle part of the (a) NE and (b) SW roofs. (c) Rafter part of the middle part of the NE roof. Condensation: the day when the condensation occurred. Temperature over 45 °C: the day when the daily maximum temperature reached over 45 °C.

5 Conclusion

This study was aimed at clarifying the quantitative relationship between airborne algal growth and the surrounding environment. The following conclusions can be drawn.
– The stripe-shaped soiling extended vertically from top to bottom on the NE and NW roofs. In contrast, soiling did not occur on the SE and SW roofs. On the NE and NW roofs, the soiling hardly increased in the summer and winter but increased from March to June and from September to November.
– The SW, SE, NW, and NE roofs, in this order, showed the highest frequency of surface

temperatures of over 45 °C because of solar radiation.

– The surface condensation occurred on all roofs from May to October, and the daily condensation time was long, especially from September to October. The frequency and period of the condensation were almost the same for all roofs (orientation).

– The surface temperature of the SE and SW roofs was higher than 45 °C during the daytime from May to November. Therefore, despite the occurrence of the condensation, the algae died owing to the high temperature, and thus soiling did not occur.

– The comparison of the rafter and air-layer parts of the NE roof showed an almost same frequency of high temperatures of over 45 °C. However, the condensation time per day at the rafter part was longer than that at the air-layer part. Therefore, the algae could grow more on the rafter part, where the soiling was first observed to occur.

Acknowledgements

ORCID

Makiko Nakajima: https://orcid.org/0000-0001-7753-4113

References

Y. Tsujimoto, N. Ohba and T. Sudoh (1992). Identification of Fresh-water Algae of External Building Walls and Study on an Evaluation Method for the Soiling by Fresh-water Algae, J. Struct. Constr. Eng. (Transactions AIJ). 433 11–17. doi:10.3130/aijsx.433.0_11.

N. Ohba and Y. Tsujimoto (1996). Soiling of external materials by algae and its prevention 1. Situation of soiling and identification of algae, Mokuzai Gakkaishi. 42 589–595.

C.C. Gaylarde and P.M. Gaylarde (2005). A comparative study of the major microbial biomass of biofilms on exteriors of buildings in Europe and Latin America, Int. Biodeterior. Biodegradation. 55 131–139. doi:10.1016/J.IBIOD.2004.10.001.

A.Z. Miller, P. Sanmartín, L. Pereira-Pardo, A. Dionísio, C. Saiz-Jimenez, M.F. Macedo and B. Prieto, (2012). Bioreceptivity of building stones: A review, Sci. Total Environ. 426 1–12. doi:10.1016/j.scitotenv.2012.03.026.

N.K. Sharma, A.K. Rai, S. Singh and R.M. Brown (2007). Airborne algae: their present status and relevance1 doi:10.1111/j.1529-8817.2007.00373.x, J. Phycol. 43 615–627. http://www.blackwell-synergy.com/doi/abs/10.1111/j.1529-8817.2007.00373.x.

W.M. Darley (1982) Algal biology: a physiological approach, Blackwell Scientific Publications.

N. Häubner, R. Schumann and U. Karsten (2006). Aeroterrestrial microalgae growing in biofilms on facades - Response to temperature and water stress, Microb. Ecol. 51 285–293. doi:10.1007/s00248-006-9016-1.

S.C. Agrawal and V. Singh (2000). Vegetative survival, akinete formation and germination in three blue-green algae and one green alga in relation to light intensity, temperature, heat shock and UV exposure, Folia Microbiol. (Praha). 45 439–446. doi:10.1007/BF02817618.

M. Nakajima, S. Hokoi, D. Ogura and C. Iba (2015). Relationship between environmental conditions and algal growth on the exterior walls of the Ninna-ji Temple, Kyoto, in: Energy Procedia. doi:10.1016/j.egypro.2015.11.149.

M. Nakajima, S. Hokoi, D. Ogura and C. Iba (2015). Modeling of algal gorwth and death on exterior walls of buildings, J. Environ. Eng. 80. doi:10.3130/aije.80.1125.

T. Martinez, A. Bertron, G. Escadeillas and E. Ringot (2014). Algal growth inhibition on cement mortar: Efficiency of water repellent and photocatalytic treatments under UV/VIS illumination, Int. Biodeterior. Biodegradation. 89 115–125. doi:10.1016/J.IBIOD.2014.01.018.

F. Gladis and R. Schumann (2011). Influence of material properties and photocatalysis on phototrophic growth in multi-year roof weathering, Int. Biodeterior. Biodegradation. 65 36–44. doi:10.1016/J.IBIOD.2010.05.014.